sciendo

DOI: 10.2478/auoc-2018-0018

Ovidius University Annals of Chemistry Volume 29, Number 2, pp. 122-125, 2018

Synthesis and structural analysis of $Ni_{0.45}Cu_{0.55}Mn_2O_4$ by Williamson–Hall and size–strain plot methods

Shashidhargouda H. R.[1] and Shridhar N. MATHAD[2,*]

Department of Physics, Tontadarya College of Engineering, Gadag, Karnataka, India
Department of Physics, K.L.E. Institute of Technology, Hubballi-580030, Karnataka, India

Abstract. This paper describes synthesis and structural properties of $Ni_{0.45}Cu_{0.55}Mn_2O_4$ nanopowder, obtained by co-precipitation route. XRD pattern reveals cubic structure with lattice parameter 8.305 Å. We report crystallite size (D), micro strain (ε), dislocation density (ρ_D), and hopping lengths (L_A and L_B). We also report preferential orientation by texture coefficients [Tc (h k l)]. The Williamson-Hall plot and stress-strain plot also employed to understand the mechanical properties of materials.

***Keywords*:** $Ni_{0.45}Cu_{0.55}Mn_2O_4$, crystallite size ($D$), micro strain ($\varepsilon$), dislocation density ($\rho_D$), texture coefficients.

1. Introduction

Mixed manganese oxides have recently evoked strong concern in various structures with different Mn valence states and Mn coordinations like in perovskites, spinels, or pyrochlores [1]. Sensors for monitoring and controlling temperature are very authoritative, our daily life, tons of industrial and laboratory applications like aerospace, automotive industries, circuit compensation and cryogenic systems etc. [2, 3]. The negative temperature coefficient (NTC) thermistors are useful for precision temperature measurements as their resistance decreases with increasing temperature [3]. The most extensively used NTC thermistor materials are nickel-manganite based semiconducting materials which exhibit the spinel-type crystal structure with the general formula AB_2O_4 [4, 5]. In the spinel structure, there are two sites available for the cations, i.e. the tetrahedral site, A-site, and the octahedral site, B-site [4]. $NiMn_2O_4$ is panoptically used in industry as the basis for the production of ceramic temperature sensors due to its electrical properties characterized by a negative temperature coefficient of the semi-conducting electrical resistance [5 - 8]. Copper plays an important role in the physical and electrical properties of nickel manganite [5, 9].

This work aimed at the synthesis of $Ni_{0.45}Cu_{0.55}Mn_2O_4$ by co-precipitation method and its characterization by XRD with special emphasis of the dislocation density (ρ_D), mechanical properties (strain), and hopping length (for tetrahedral L_A and octahedral site L_B) of synthesized nickel copper manganite.

2. Experimental

Nano sized nickel copper manganites were synthesized by low cost co-precipitation method [10] from precursors like nickel chloride ($NiCl_2{\cdot}6H_2O$, 97%,), manganese chloride ($MnCl_2{\cdot}4H_2O$, 99%,) and copper chloride ($CuCl_2{\cdot}2H_2O$, 99%), all three of AR grade made by Burgoyne Burbridges & Company, Mumbai, India. The reagents were weighed for a desired stoichiometric ratio and dissolved in distilled water. The mixture was stirred for 1 hour by using a magnetic stirrer to get liquid solution at room temperature (300 K). Then ammonia (NH_3 25%, extra pure Sp. gr. 0.91, Fisher Scientific, Mumbai) was added drop wise with a pipette to get a desired pH value and stirred for another 1 hour. The brown solution contained nano nickel copper manganite which was washed repeatedly by adding distilled water and filtered by using AR grade filter paper, as shown in Fig. 1. The paste finally left to dry at room temperature. To get final product, the dry paste was calcinated at 600°C for 4 hours in a muffle furnace, using an alumina crucible. The black powder left is the nano nickel copper manganite sample. XRD analysis of synthesized nickel copper manganite was carried out by using a Bruker AXS D8 Advance instrument (λ = 1.5406 Å, Detector Si(Li) PSD from STIC, Cochin).

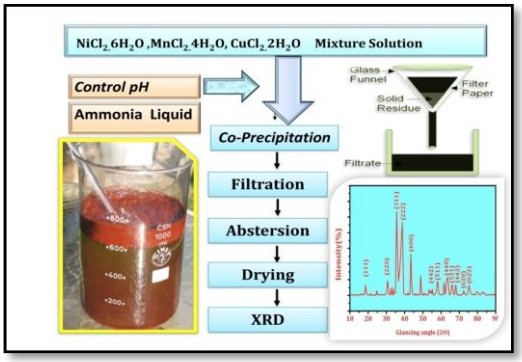

Figure 1. Schematic of synthetic procedure and flow chart of co-precipitation method.

3. Results and discussion

The cubic spinel structure of nickel copper manganite is confirmed by the diffraction pattern shown in Figure 2. The diffraction pattern was indexed using JCPDS #00-084-0542, demonstrating the synthesis of nickel copper manganite. The diffraction pattern analysis is done by

* Corresponding author. *E-mail address:* physicssiddu@gmail.com (Shridhar N. Mathad)

using (1 1 1), (2 2 0), (3 1 1), (2 2 2), (4 0 0), (4 4 2), (5 1 1), (4 4 0), (5 3 1), (6 2 0) and (6 2 2) reflection planes, which confirmed the formation of a cubic spinel structure. Miller indices (*h k l*) and lattice parameter (*a*) are tabulated in Table 1. The peaks positions and relative intensities match the tabulated values for $NiMn_2O_4$. XRD pattern reveals cubic spinel structure phase (space group: Fd3m) and crystalline nature with lattice constant *a* = 8.305 Å.

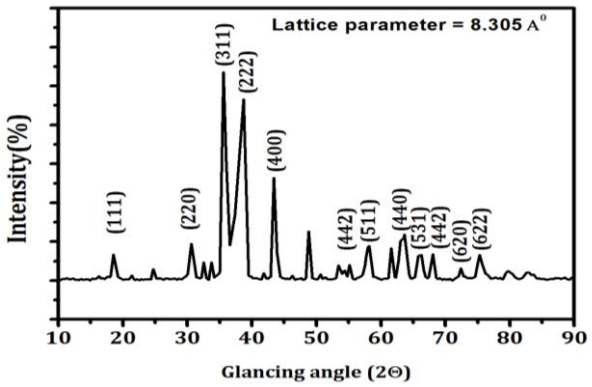

Figure 2. XRD pattern of $Ni_{0.45}Cu_{0.55}Mn_2O_4$

Table 1. Miller indices (*h k l*) and lattice parameter (a)

2θ	*d* [Å]	Miller indices (*h k l*)	Lattice constant (*a*) [Å]
18.492	4.79421	1 1 1	8.303
30.559	2.92305	2 2 0	8.267
36.009	2.49217	3 1 1	8.265
37.357	2.40526	2 2 2	8.332
43.407	2.08301	4 0 0	8.332
55.132	1.66454	4 2 2	8.154
58.184	1.58428	5 1 1	8.232
63.099	1.47218	4 4 0	8.237
65.827	1.41762	5 3 1	8.386
66.328	1.40812	4 4 2	8.448
72.412	1.30406	6 2 0	8.247

Crystallite size *D* was calculated using the Debye–Scherer equation [10]:

$$D = \frac{0.9\lambda}{\beta cos\theta} \qquad (1)$$

where λ is the wavelength of used radiation, β is the full width half maximum (FWHM) of diffraction peak, and θ is the Bragg angle. The lattice parameter of synthesized cubic nickel copper manganite found as *a* = 8.305 Å, the unit cell volume is 572.84 $Å^3$ and average crystallite size *D* is 39.8 nm, as presented in Table 2.

Table 2. Lattice parameter (*a*), volume (*V*), strain (ε), crystallite size (*D*) and hopping lengths (L_A and L_B)

a [Å]	a^3 [$Å^3$]	ε	*D* [nm]	ρ_D [m^2]	L_A [Å]	L_B [Å]
8.305	572.8	0.0915	39.8	7.38385×10^{18}	3.596	2.94

The dislocation is a crystallographic defect (irregularity) within a crystal structure, which strongly influences the material properties. Dislocation density is the number of dislocations in a unit volume of crystalline material. Dislocation density ρ_D and micro strain ε were calculated from [10]:

$$\rho_D = 1/D^2 \qquad (2)$$

$$\varepsilon = \beta \cos\theta / 4 \qquad (3)$$

$$\rho_D = \frac{15\varepsilon}{aD} \qquad (4)$$

The distances between magnetic ions (hopping length) in site A (tetrahedral) and site B (octahedral) were calculated by using the following relationships (5), being equal to 3.596 Å and 2.94 Å:

$$L_A = \frac{a\sqrt{3}}{4} \text{ and } L_B = \frac{a\sqrt{2}}{4} \qquad (5)$$

Quantitative information concerning the preferential crystal orientation can be obtained from the texture coefficient, *T*c (*h k l*) [11]. The reflection intensities from each XRD pattern contain information related to the preferential growth of phases in polycrystalline material. The degree of orientation in crystal planes can be found from the expression:

$$Tc\ (h\ k\ l) = \frac{\frac{I(h\ k\ l)}{I_0(h\ k\ l)}}{(\frac{1}{N})\Sigma\frac{I(h\ k\ l)}{I_0(h\ k\ l)}} \qquad (6)$$

where *I* and I_0 stand for the observed and standard intensities and *N* is number of peaks. Texture analysis is tabulated in Table 3.

Table 3. Texture coefficients of planes (*h k l*)

h k l	*T*c (*h k l*)
1 1 1	0.678
2 2 0	0.396
3 1 1	0.72
2 2 2	3.054
4 0 0	1.774
4 2 2	0.625
5 1 1	0.192
4 4 0	0.413
6 2 0	1.829

We would realize that the *T*c of (2 2 2) and (6 2 0) are 3.054 and 1.829 respectively and showed strong preferential orientation about the (2 2 2) plane compared to other planes.

Lattice strain η and average crystalline size *D* were calculated using the Williamson–Hall equation [12]:

$$\frac{\beta cos\theta}{\lambda} = \frac{1}{D} + \frac{\eta sin\theta}{\lambda} \qquad (7)$$

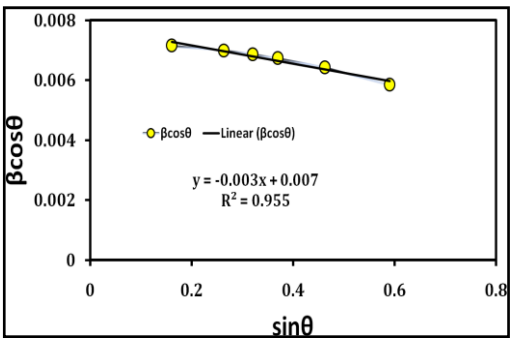

Figure 3. Williamson–Hall plot of $\beta\cos\theta$ *vs*. $\sin\theta$ Ni-Cu-Mn-O

The above equation is written in the format $y = mx + c$ where $m = \eta$ and $c = 1/D$, so that the linear plot of $\beta\cos\theta$ *vs*. $\sin\theta$ gives the slope as lattice strain η and the intercept as $1/D$ as shown in Fig. 3. From the graph calculated average crystallite size (D) was 142 nm and lattice strain $\eta = 0.003$ to agree with the above calculations.

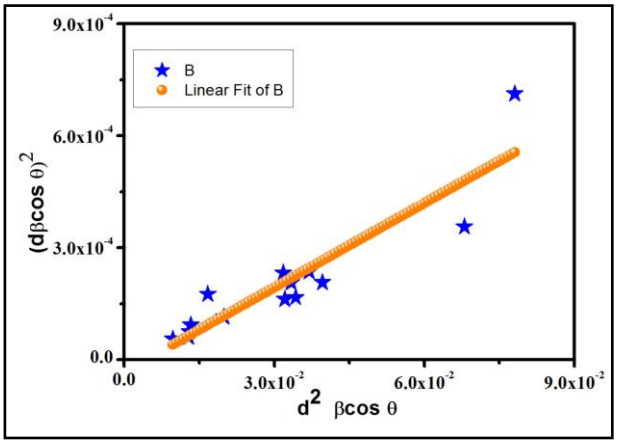

Figure 4. Size-strain plot of $(d\beta\cos\theta)^2$ *vs*. $d^2\beta\cos\theta$ of $Ni_{0.45}Cu_{0.55}Mn_2O_4$

The "size-strain plot" (SSP) is best tool to empathize the isotropic nature and micro-strain contribution. The judgment of the size-strain parameters can be obtained by considering an average (SSP), which has the benefits that less weight is given to data from reflections at high angles, where the precision is usually lower which is shown in Figure 4. We presume that the "crystallite size" profile is represented by a Lorentzian function and the "strain profile" by a Gaussian function [12, 13].

Accordingly, we have:

$$(d_{hkl}\beta_{hkl}\cos\theta)^2 = \frac{K.\lambda}{D}(d_{hkl}^2\beta_{hkl}\cos\theta) + \left(\frac{\varepsilon}{2}\right)^2 \quad (8)$$

where K is a constant that depends on the shape of the particles (for spherical particles $K = 3/4$)

In this case, the comparison between W-H plot and SSP has been reported in Table 4.

Table 4. Comparative values of crystallite size (D), micro strain (ε), and dislocation density (ρ_D)

Crystallite size *D* [Å]	From equation	From W-H graph	From SSP method
	398	142	155
Micro strain *ε*	From equation	From W-H graph	From SSP method
	0.0016	0.003	0.011
Dislocation density ρ_D [m^{-2}]	From Eq (3)	From Eq (4)	
	1.6992 x 10^{15}	1 x 10^{15}	

4. Conclusion

Nano-sized nickel copper manganite has been synthesized by cost effective co-precipitation method. Synthesized nano particles had a cubic spinel structure with average lattice parameter $a = 8.305$ Å and average crystallite size $D = 39.8$ nm. The lattice strain of $Ni_{0.45}Cu_{0.55}Mn_2O_4$ was found to be 0.092. We would realize that the *T*c of (2 2 2) is 3.054 showed strong preferential orientation about the (2 2 2) plane compared to other planes. We have also correlated crystalline structure by W-H plot and SSP method.

Conflict of interest

The authors confirm that this article content has no conflicts of interest.

References

[1]. B.P. Boucher, R. Buhl, M. Perrin, Etude cristallographique du manganite spinelle cubique $NiMn_2O_4$ par diffraction de neutron, Acta Crystallographica B 25 (1969) 2326.

[2]. R. N. Jadhav, S. N. Mathad, V. Puri, Studies on the properties of $Ni_{0.6}Cu_{0.4}Mn_2O_4$ NTC ceramic due to Fe doping, Ceramics International 38 (2012) 5181–5188. DOI: 10.1016/j.ceramint.2012.03.024

[3]. M.N. Muralidharan, P.R. Rohini, E.K. Sunny, K.R. Dayas, A. Seema, Effect of Cu and Fe addition on electrical properties of Ni–Mn–Co–O NTC thermistor compositions, Ceramics International 38 (2012), 6481–6486. DOI: 10.1016/j.ceramint.2012.05.025

[4]. J. Fraden, Handbook of Modern Sensors Physics, Designs, and Applications, Springer Science Business Media, New York 2010.

[5]. R. N. Jadhav, S. N. Mathad, V. Puri, Properties of fritless $Ni_{0.6}Cu_{0.4}Fe_yMn_{2-y}O_4$ NTC ceramic thick films, Physica Scripta 87 (2013) 065801-08. DOI: 10.1088/0031-8949/87/06/065801

[6]. J.L. Martin de Vidales, P. Garcia-Chain, R.M. Rojas, E. Vila, O. Garcia-Martinez, Preparation and characterization of spinel-type Mn–Ni–Co–O negative temperature coefficient ceramic thermistors, Journal of Materials Science 33 (1998) 1491–1496. DOI: 10.1023/A:1004351809932

[7]. S. Fritsch, J. Sarrias, M. Brieu, J.J. Couderc, J.L. Baudour, E. Snoeck, A. Rousset, Correlation between the structure, the microstructure and the electrical properties of nickel manganite negative temperature coefficient (NTC) thermistors, Solid State Ionics 109 (1998) 229-237. DOI: 10.1016/S0167-2738(98)00080-0

[8]. A.V. Salker, S.M. Gurav, Electronic and catalytic studies on $Co_{1-x}Cu_xMn_2O_4$ for CO oxidation, Journal of Materials Science 35 (2000) 4713–4719. DOI: 10.1023/A:1004803123577

[9]. S.S. Yattinahalli, S.B. Kapatkar, S.N. Mathad, Synthesis and structural characterization of nano – manganese ferrites, Journal of Nano- and Electronic Physics 7 (2015) 04096-1 - 04096-3.

[10]. U. Holzwarth, N. Gibson, The Scherrer equation versus the "Debye-Scherrer equation", Nature Nanotechnology 6 (2011) 534. DOI: 10.1038/nnano.2011.145.

[11]. S.N. Mathad, R.N. Jadhav, N.D. Patil, V. Puri, Structural and mechanical properties of Sr^{+2} doped bismuth manganite thick films, International Journal of Self-propagating High Temperature Synthesis 22 (2013) 180-184.

[12]. A.B. Kulkarni, S.N. Mathad, Synthesis and structural analysis of Co-Zn-Cd ferrite by

Williamson-Hall and size-strain plot methods, International Journal of Self-Propagating High-Temperature Synthesis 27 (2018) 37–43. DOI: 10.3103/S106138621801003X

[13]. Y.T. Prabhu, K.V. Rao, V.S.S. Kumar, B.S. Kumari, X-ray analysis by Williamson-Hall and size-strain plot methods of ZnO nano particles with fuel variation, World Journal of Nano Science and Engineering 4 (2014) 21–28. DOI: 10.4236/wjnse.2014.41004

Received: 10.10.2018
Received in revised form: 07.11.2018
Accepted: 27.11.2018